Available online at www.sciencedirect.com
ScienceDirect
Geochimica et Cosmochimica Acta 72 (2008) 3446–3459
Geochimica et Cosmochimica Acta
www.elsevier.com/locate/gca

Ra and Th adsorption coefficients in lakes—Lake Kinneret (Sea of Galilee) "natural experiment"

Boaz Lazar [a,*], Yishai Weinstein [b], Adina Paytan [c], Einat Magal [d], Debbie Bruce [a], Yehoshua Kolodny [a]

[a] *Institute of Earth Sciences, The Hebrew University of Jerusalem, 91904 Jerusalem, Israel*
[b] *Department of Geography and Environment, Bar Ilan University, Israel*
[c] *Department of Earth and Planetary Sciences, UC Santa Cruz, Santa Cruz, CA 95064, USA*
[d] *The Geological Survey of Israel, 30 Malchei Israel St., Jerusalem 95501, Israel*

Received 14 May 2007; accepted in revised form 15 February 2008; available online 21 May 2008

Abstract

The adsorption rate constants of Ra and Th were estimated from empirical data from a freshwater lake and its feeding saline springs. We utilized the unique setting of Lake Kinneret (Sea of Galilee, northern Israel) in which most of the Ra and Th nuclides are introduced into the lake by saline springs with high ^{226}Ra activities and a high ^{224}Ra/^{228}Ra ratio of 1.5. The mixing of the Ra enriched saline waters and freshwater in the lake causes the ^{224}Ra/^{228}Ra ratio to drop down to 0.1 in the Kinneret due to preferential adsorption of ^{228}Th. These conditions constitute a "natural experiment" for estimating adsorption rates. We developed a simple mass-balance model for the radionuclides in Lake Kinneret that accurately predicted the Ra isotope ratios and the ^{226}Ra activity in the lake. The model is comprised of simultaneous equations; one for each radionuclide. The equations have one input term: supply of radionuclides from the saline springs; and three output terms: adsorption on particles in the lake, radioactive decay and outflow from the lake. The redundancy in the analytical solutions to the mass balance equations for the relevant nuclides constrained the values of Ra and Th adsorption rate constants to a very narrow range. Our results indicate that the adsorption rate constant for Ra is between 0.005 d^{-1} and 0.02 d^{-1}. The rate constant for Th is between 0.5 d^{-1} and 1 d^{-1}, about fifty to a hundred times higher. The estimated desorption rate coefficient for Ra is about 50–100 times larger than its adsorption rate constant. The mass-balance equations show that the residence times of all Ra isotopes (^{226}Ra, ^{228}Ra,^{223}Ra, ^{224}Ra) and of ^{228}Th in the lake are about 95, 92, 14, 6 and 1 d, respectively. These residence times are much shorter than the residence time of water in the lake (about 5.5 y). The steady state activity ratios in Lake Kinneret depend mainly on the adsorption rate constants, decay constants, the outflow rate from the lake and the activity ratios in the saline springs. The activity ratios are independent of the saline springs flow rate.

1. INTRODUCTION

The radioactive decay series of uranium and thorium include several elements with extremely contrasting chemical properties, ranging from inert gases (He, Rn), very water-soluble species (U as uranyl ion) and extremely particle reactive ions Th(IV). The application of the short lived nuclides in the U–Th series for estimating various geochemical processes, such as the rate of particle fluxes in oceans and lakes, groundwater age and transport in aquifers, depends markedly on the rate constants for adsorption (and desorption) of the various nuclides onto different solids (Krishnaswami et al., 1982; Bacon and Anderson, 1982; Krishnaswami et al., 1991; Luo and Ku, 1999; Chase et al., 2002). The high tendency of Th to adsorb onto solid surfaces has a major role in modifying the radioactive mass

* Corresponding author. Fax: +972 2 566 2581.
E-mail addresses: boaz.lazar@huji.ac.il (B. Lazar), weinsty@mail.biu.ac.il (Y. Weinstein), apaytan@ucsc.edu (A. Paytan), einat.magal@mail.gsi.gov.il (E. Magal), gdbruce@gmail.com (D. Bruce), kolodny@vms.huji.ac.il (Y. Kolodny).

0016-7037/$ - see front matter © 2008 Elsevier Ltd. All rights reserved.
doi:10.1016/j.gca.2008.02.027

balance equilibrium equations even of very short lived daughter nuclides. This tendency was acknowledged as early as the late 1940's when substantial depletion of ^{226}Ra in seawater (by a factor of about 10) from its great grandparent ^{238}U was attributed to preferential removal of Th into the sediments (see Koczy, 1958 and references therein). Ra isotopes, products in the same U–Th series decay chains as Th, are however more soluble than Th (Moore, 1992; Krest and Harvey, 2003). ^{226}Ra, being more "mobile" (than its parent ^{230}Th) diffuses upwards from the sediments to the overlying water, making the seafloor the principal source of ^{226}Ra in the open ocean. The difference in chemical behavior of nuclides in the U–Th decay chain has been utilized extensively. For example ^{234}Th measurements have been applied to a broad range of marine problems such as particle cycling and sediment dynamics (Roy-Barman et al., 2002; Waples et al., 2006). A combination of Ra and Th isotopic studies was applied to problems related to radioactive waste disposal (Allard et al., 1979; EPA, 1999, 2004), groundwater and brine research (Zukin et al., 1987; Krishnaswami et al., 1991) lacustrine studies (Kraemer, 2005) and in recent years to the fast growing field of submarine groundwater discharge (SGD) (Moore, 1996, 1999; Rama and Moore, 1996). In all these fields the knowledge of the adsorption–desorption properties of Ra and Th in different aquatic systems is of outmost importance.

Indeed, much effort has been devoted to estimating the adsorption–desorption rate constants (k) and the equilibrium distribution coefficients (K_d) of both elements between various solids and water of different salinities. Distribution coefficients and rate constants were determined from field measurements—comparing seawater to particulate matter therein (Bacon and Anderson, 1982; Honeyman et al., 1988; Chase et al., 2002), groundwater measurements (Krishnaswami et al., 1982), saline brines (Krishnaswami et al., 1991) and laboratory studies (Allard et al., 1979; Webster et al., 1995). Webster et al. (1995) studied experimentally the dependence of Ra isotope partitioning between sediments of different grain sizes, and solutions of several salinities. They also examined the effect of sediment/water ratio upon the partition coefficient of Ra. The strongest factor influencing Ra adsorption and desorption was shown to be the salinity of the aqueous solution. When seawater is diluted tenfold, desorption of Ra decreases by a factor of about 10.

The study of radium in lakes has its origin with the landmark paper by Emerson and Hesslein (1973) that studied the behavior of artificially added ^{226}Ra into a small lake in Canada and conducted experiments to estimate the radium uptake rate on the lake's particulate organic matter. They found that ca. 90% of the Ra added to the lake was removed from the water within less then a month. The radium was taken up by algal detrital material (particulate organic matter—POM) in the littoral zone. The laboratory experiments showed that Ra was effectively adsorbed on POM regardless of whether the organic matter was preboiled, the experimental vessel was poisoned or highly enriched with Ba (a potential competitor to Ra for adsorption sites). Calculations of the Ra adsorption rate constant from their published experimental data (Table on page 1488, Emerson and Hesslein, 1973) yields an adsorption rate constant of ca. 3 d^{-1} whereas calculating their reported adsorption half life (Fig. 3 in Emerson and Hesslein, 1973) yield an adsorption rate constant in the range of 700–3000 d^{-1}. These estimates are extremely high compared to all other estimates (see references cited above). Recently, the residence time of ^{234}Th in Lake Michigan was estimated to be 1 d (Waples et al., 2004), which is much shorter than its mean life (34.8 d). This indicates that Th geochemistry in the lake is governed by adsorption, not by decay and hence the Th adsorption rate constant in Lake Michigan is about 1 d^{-1}. The adsorption rate constant of Th is higher than that of Ra by a factor of about 100 suggesting that the Ra adsorption rate constant should be around 0.01 d^{-1} or up to 6 orders of magnitude lower than the estimates of Emerson and Hesslein (1973). The high estimates may stem from the high POM to water ratio in the experimental vessels, however, these conflicting results suggest that the Ra adsorption rate constant in lakes remains poorly constrained.

The present study is an attempt to estimate the adsorption rate constants of Ra and Th in freshwater, using for this purpose the unique characteristics of Lake Kinneret (The Sea of Galilee). The Kinneret receives most of its salts including Ra and Th from the saline springs, which discharge into the lake (Kolodny et al., 1999; see below and Fig. 1). The mobility of the radionuclides decreases drastically as these very saline, high radioactivity brines flow into freshwater. The major trigger for the initiation of the present study has been our observation that whereas in the inflowing saline springs the ^{224}Ra/^{228}Ra activity ratio is about 1.5, the ratio in the lake is around 0.1. We suggest that this sharp decrease is due to preferential removal of ^{228}Th, the parent of ^{224}Ra. We then used this sharp break in the radioactive decay chain as a "natural experiment" for quantifying the removal of both ^{228}Th and the Ra isotope "quartet" onto particles in terms of adsorption rate constants.

Our study is the opposite case of the classical scenario, in which freshwater brings particles into seawater medium; in such a scenario all Ra isotopes, and to a lesser degree Th undergo desorption and solubilization. In Lake Kinneret the inverse happens: high salinity water rich in Ra isotopes flows into a freshwater lake, and both Ra, and to a greater degree Th, are removed from solution mainly by adsorption onto Lake Kinneret particles which are settling to the sediment. In our study we deal with the four Ra isotopes ^{226}Ra ($T_{1/2} = 1600$ y), ^{228}Ra ($T_{1/2} = 5.75$ y) ^{224}Ra ($T_{1/2} = 3.7$ d) and ^{223}Ra ($T_{1/2} = 11.4$ d). We also consider in some detail one thorium isotope, ^{228}Th ($T_{1/2} = 1.91$ y).

1.1. Lake kinneret; background

Lake Kinneret (The Sea of Galilee, or Lake Tiberias) is located in northeast Israel in the northern part of the Dead Sea Transform (the Jordan Rift Valley), about 200 m below sea level. It has an area of about 160 km^2, a volume of 4.1×10^9 m^3, and its maximum depth in its center is about 45 m. It is a freshwater lake (TDS $\cong$ 690 mg L^{-1}, $Cl^- \cong$ 250 mg L^{-1}). The major source of water to the lake is the Jordan River in the north and the present day water output is mainly through diversion into the Israeli National

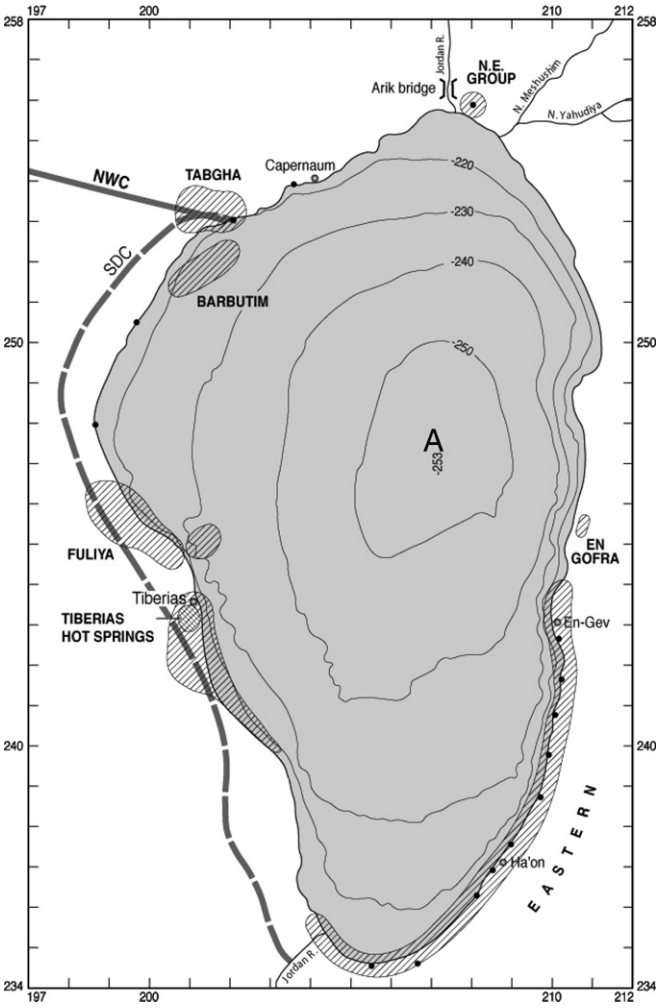

Fig. 1. Map of Lake Kinneret indicating water inputs in the north (mainly Jordan River); water output (mainly the National Water Carrier, marked NWC on the map); and the major saline springs groups (all on the west coast): Tiberias Hot Springs (including the groups called Main and Roman springs, see Fig. 2), the Fuliya group (including the wells, see Table 1 and text), and the Tabgha group (including Ma'ayan Matok and Sartan Iver springs, see Fig. 2). The Kinneret is represented in the study by station A (middle of the lake). Presently a large percentage of the on-land springs is being diverted south of the lake by the Spring Diversion Carrier (marked SDC on the map). Contours are depth in meters. Major spring areas are shaded in diagonal raster.

Water Carrier (Fig. 1). The water residence time in the Kinneret is about 5.5 y (data in Kolodny et al., 1999). The salts in Lake Kinneret are almost entirely contributed by several groups of saline springs, some of them onshore, most of them submerged (Fig. 1). The exact location of most of these unmonitored springs is not known (Kolodny et al., 1999; Nishri et al., 1999), but observations from recent low lake level years point to the Fuliya area (Fig. 1) as a major salt source. The fraction of different ions supplied to the lake from the saline springs varies: it is about 50% for Mg, 85% for Na and 95% for bromide (Kolodny et al., 1999). The largest known onshore springs are located on the western shore of the lake, and appear in three discreet groups, from south to north: Tiberias Hot Springs, the Fuliya Group, and the Tabgha group (Fig. 1). Element by element mass balance calculations, as well as a simulation of the Lake's evolution since the diversion of some saline springs in 1964, suggests that the Fuliya and possibly some Tabgha type brines are most representative of the overall chemical composition of the unmonitored submerged seepages into the Lake (Kolodny et al., 1999). It was estimated that at their present flow rate, the saline springs (monitored + unmonitored) can fill a volume equivalent to the Kinneret in ca. 60 y (calculated from data in Kolodny et al., 1999). The considerable difference in residence times of water and salts in the lake (about 5 y and 10 y, respectively) stems from their different sources. While the saline springs supply most of the salts, most of the water (H_2O) is supplied by the Jordan River and runoff (see above and Fig. 1).

All the saline springs in the Dead Sea Rift valley have very high but variable content of ^{222}Rn and Ra isotopes (Table 1). Generally, the activity of these radionuclides increases with salinity, as is the case for all saline springs in the rift valley (Mazor, 1962; Moise et al., 2000). The radio-geochemistry of the brines has been well studied (Mazor, 1962; Moise et al., 2000). Moise et al. (2000) reported a systematic survey of the springs' general chemistry as well

Table 1
Activities and activity ratios of the relevant nuclides in Lake Kinneret and its saline spring sources (see text), *n* indicates number of samples analyzed

	^{223}Ra (dpm m^{-3})	^{224}Ra (dpm m^{-3})	^{226}Ra (dpm m^{-3})	^{222}Rn (dpm L^{-1})	Cl$^-$ (mg L^{-1})	$\frac{^{226}Ra}{Cl^-}$ (dpm g^{-1})	$\frac{^{228}Ra}{^{226}Ra}$	$\frac{^{224}Ra}{^{223}Ra}$	$\frac{^{224}Ra}{^{228}Ra}$	$\frac{^{222}Rn}{^{226}Ra}$
Kinneret surface, 0–10 m	1.3 ± 0.5, $n = 2$	5.4 ± 2.2, $n = 2$	630 ± 330, $n = 8$	3.7 ± 1.6, $n = 6$	260 ± 30	2 ± 1	0.17 ± 0.03, $n = 9$	4 ± 2, $n = 2$	0.05 ± 0.03, $n = 2$	6 ± 5
Kinneret bottom, 30–40 m	1.4 ± 0.1, $n = 1$ [a]	16 ± 1.6, $n = 1$ [a]	550 ± 120, $n = 12$	1.8 ± 0.6, $n = 6$	260 ± 30	2 ± 1	0.17 ± 0.08, $n = 7$	11 ± 2, $n = 1$ [a]	0.2 ± 0.1, $n = 1$ [c]	3 ± 2
Tabgha	—	8800 ± 1500, $n = 2$	18,000–38,000, $n = 5$	9000 ± 1000, $n = 6$	1500–3000	13 ± 3	0.21 ± 0.06, $n = 6$	—	1.5 ± 0.1, $n = 2$	250–500
Fuliya springs	110 ± 8, $n = 1$ [a]	1000–6000, $n = 4$ [b]; 800	7400–57,000, $n = 6$	9500 ± 160, $n = 1$	1200–8700	6.2 ± 0.3	0.13 ± 0.02, $n = 6$	7.8 ± 0.6, $n = 1$ [a]	1.8 ± 0.2, $n = 4$	170–1300
Fuliya springs + wells	—	1000–40,000, $n = 8$	7400–110,000, $n = 10$	2400–10,200	1200–17,000	6.2 ± 0.1	0.14 ± 0.5, $n = 10$	—	1.6 ± 0.3, $n = 8$	90–320
Tiberias Hot Springs	—	20,000 ± 2300, $n = 6$	250,000 ± 40,000, $n = 13$	9500 ± 3400, $n = 12$	18,400 ± 400	11–18	0.08 ± 0.02, $n = 13$	—	1.0 ± 0.2, $n = 6$	40 ± 20

Ranges are given for nuclides showing positive correlation with Cl$^-$ concentration that is variable in different springs from each group. The row for "Fuliya springs + wells" was added to the table because the brines in the wells are more concentrated (and more radioactive) than the springs. These well waters are closer to the composition of the saline end-member (Moise et al., 2000; see also Fig. 2). The spring data in the table were averaged with those from Moise et al. (2000); Kinneret ^{226}Ra and ^{222}Rn data were averaged with Nishri and Stiller (1997).

[a] Counting error only, all other errors are standard deviations of a mean.

[b] Values obtained by calculating the proper activity ratio measurements.

[c] The Kinneret bottom ^{224}Ra/^{228}Ra ratio may represent a submerged spring or diffusion from bottom sediment (see discussion in chapter 3 paragraph 4, above), we however used the weighted average of Kinneret surface value as representative of the ^{224}Ra/^{228}Ra ratio of Lake Kinneret (see Fig. 9).

as activities of ^{222}Rn and ^{226}Ra/^{228}Ra activity ratios in all the springs along the Kinneret shore. The ^{224}Ra/^{228}Ra activity ratios were also measured in most of the springs. A summary of the relevant results as well as chlorinity for the saline springs is given in Table 1.

New data obtained in the present study include measurements of the "Ra quartet" isotopes in the lake, the saline spring Fuliya-2 (a spring on the lake shore that drains directly into the lake) and a transect of three samples conducted between that spring's inflow and Station A, located at about the central point of the Lake (Fig. 1). We used the combined data set in this "natural adsorption experiment" to estimate the adsorption–desorption rate constants (k) and the equilibrium distribution coefficients (K_d) of Ra and Th in a freshwater lake.

2. ANALYTICAL

Part of the data used in this study has been previously reported. The ^{222}Rn and ^{226}Ra in saline springs water are quoted from Moise et al. (2000) who measured the activities by the ^{222}Rn emanation technique (Mathieu et al., 1988). ^{222}Rn was determined by α counting as soon as possible after sampling and ^{226}Ra after achieving radioactive equilibrium with ^{222}Rn in a sealed bottle. In addition, we measured, using the same methods, ^{222}Rn, ^{226}Ra, both at the mouth of the Fuliya-2 spring (Fig. 1), and in several localities in the lake. ^{228}Ra/^{226}Ra and ^{224}Ra/^{228}Ra activity ratios of these samples were measured by γ-spectrometry using a high purity germanium (HPGe) detector. Ra was adsorbed on Mn-coated acrylic fibers, stripped and co-precipitated with $BaSO_4$ (Curie and Laborde, 1903) and the $BaSO_4$ subsequently counted (Moore et al., 1985). Water was not filtered prior to passing through the Mn-coated fibers, but passing a similar amount of water through an acrylic fiber without Mn coating ("white fiber"), yielded counts that did not exceed background. We concluded that the acrylic fibers did not retain particulate matter and the adsorbed Ra represents only the dissolved phase. The short lived Ra isotopes adsorbed on similar fibers were measured in the Fuliya-2 spring and in several localities in the lake as soon as possible after sampling using a delayed coincidence counter (RaDeCC; Moore and Arnold, 1996). Additional ^{226}Ra, ^{228}Ra, and two ^{224}Ra/^{228}Ra ratios in Lake Kinneret were measured by the same methods during the M.Sc. thesis of Bar-Giora Magal (2000). In order to minimize error, most of the ^{224}Ra and ^{223}Ra were counted for about one day with typical counting error for ^{224}Ra of less then ±5% and for ^{223}Ra of less then ±10%. The summary of all data is given in Table 1 and in Figs. 2 and 3.

3. THE BEHAVIOR OF Ra ISOTOPES IN THE SALINE SPRINGS AND IN LAKE KINNERET

The Cl$^-$ concentration in the saline springs varies considerably from about 1500 and up to almost 19,000 mg L^{-1} (Table 1, Fig. 2a). The most obvious feature observed in the saline springs is that Ra activity is positively well correlated with Cl$^-$ (Fig. 2a), particularly for the Fuliya group. (^{226}Ra (dpm m^{-3}) = 6.2 Cl$^-$ (mg L^{-1}); $R^2 = 0.997$). On these plots

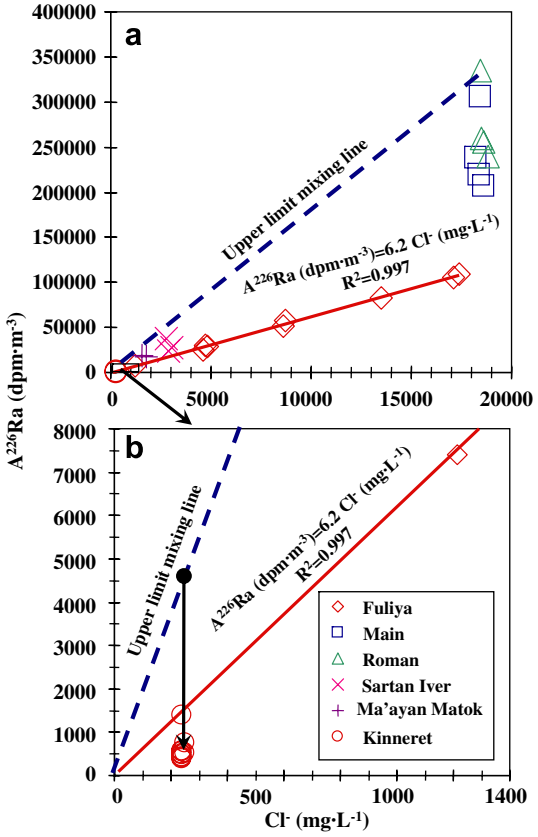

Fig. 2. Activity of ^{226}Ra as a function of Cl^- in the saline springs (most data from Moise et al., 2000) and Lake Kinneret (data from Nishri and Stiller, 1994, this study). a—Salinity range 0-20,000 mg L^{-1};b—blow up of (a) for the salinity range 0–1400 mg L^{-1}. The best fit line was drawn through the data for the Fuliya group. Tabgha group (Maayan Matok and Sartan Iver) data points plot close to that line while those of the Tiberias H.S. group plot above it. The "Upper limit mixing line" is the dilution line of the sample with the highest $^{226}Ra/Cl^-$ ratio. Note that 20 out of 21 Kinneret samples plot well below the lower (Fuliya) dilution line.

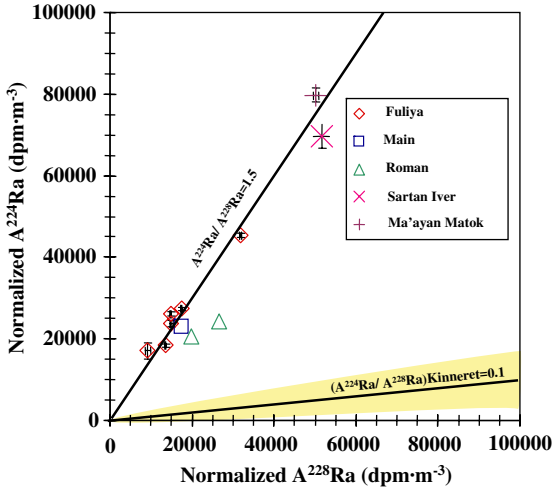

Fig. 3. Cl^- Normalized activity of ^{224}Ra versus Cl^- normalized activity of ^{228}Ra in the saline springs (most data from Moise et al., 2000). The activities were multiplied by a ratio of 20,000 mg L^{-1} to Cl^- in the sample. 20,000 mg L^{-1} was chosen because it is about the highest salinity end-member of the saline springs. Note that a line of slope 1.5 was drawn through the data rather then a best fit (see text). The lower Lake Kinneret line (data from this study) represents the $^{224}Ra/^{228}Ra$ of the lake (Table 1). The shadowed segment around the Kinneret line represents the uncertainty of the ratio.

the Fuliya group includes one spring (Fuliya 5) and three wells, referred to by Moise et al. (2000) as Kinneret-5—pumped; Kinneret-artesian and Kinneret-10; the latter was sampled at three depths. The Fuliya correlation line indicates mixing of the saline spring water with low Ra fresh groundwater (Moise et al., 2000). The two springs from the Tabgha group (Sartan Iver and Ma'yan Matok springs; Figs. 1, 2a) plot somewhat above the Fuliya correlation line. The Tiberias Hot Spring group (Main and Roman springs; Figs. 1, 2a) have relatively constant and high salinity with varying ^{226}Ra activities, all well above the Fuliya correlation line. To determine the maximum possible ^{226}Ra activity in the lake, assuming conservative behavior of ^{226}Ra, we extrapolated from the highest ^{226}Ra value in the Roman springs to the salinity of Lake Kinneret; we define this as the upper limit mixing line (Fig. 2a).

The activity of all Ra isotopes in Lake Kinneret (mid-lake, Station A, see Fig. 1) is considerably lower than in the saline springs (Table 1, Fig. 2a, b for ^{226}Ra) and is well below the extrapolated Fuliya trend that represents the lowest $^{226}Ra/Cl^-$ in the saline springs and certainly well below the extrapolated upper limit mixing line (Fig. 2b). The activity of ^{226}Ra in the lake is about 600 dpm m^{-3} with an exception of one analysis (out of 21, see Table 1), which plots right on the Fuliya trend. The lower than expected ^{226}Ra activity in the lake compared to the extrapolated conservative mixing trend indicates a net loss of 60% to 90% of ^{226}Ra. The lower value of 60% applies to a removal of Ra assuming an input composition similar to Fuliya group springs, the higher value assuming the input is closer to Tiberias Hot Springs values. Given the long half life of ^{226}Ra (ca. 1600 y) compared to the short residence time of water and salts in the lake (about 5 y and 10 y, respectively), radioactive decay cannot explain this loss suggesting that adsorption of Ra on particles is a major output term for ^{226}Ra in Lake Kinneret.

^{224}Ra is very well linearly correlated with ^{228}Ra, (both members of the ^{232}Th decay series) in the saline springs (Fig. 3). The slope of the ^{224}Ra versus ^{228}Ra correlation line is practically indistinguishable from the expected *transient* equilibrium value for the $^{228}Th/^{228}Ra$ activity ratio of 1.5 (e.g., Evans, 1955, p. 482–483; Davidson and Dickson, 1986). Thus, it appears that ^{228}Th remained in contact with the brine for a long time (ca. 12 y), sufficient to achieve transient equilibrium with ^{228}Ra (its parent) and *secular* equilibrium with its short lived daughter ^{224}Ra ($T_{1/2} = 3.7$ d). Long time contact can be achieved either by ^{228}Th remaining dissolved or by its deposition on the walls of the spring's conduits, or by a combination of both. Apparently, the brine emerges to the surface rather rapidly (within ca. 1 day), or else, once disconnected from the ^{228}Th, the activity of ^{224}Ra would decay and the $^{224}Ra/^{228}Ra$ activity ratio would decrease below the observed ratio of 1.5. Dissolved ^{228}Th was detected in the low salinity spring, Fuliya 2 (ca. 3000 mg Cl L^{-1}) both by RaDeCC and by a-spectrometry. We

analyzed the lower salinity spring Fuliya 2 because the saline (17,000 mg Cl L^{-1}) well is inaccessible. ^{228}Th was detected by the presence of a significant ^{224}Ra signal six months after sampling. The estimated ^{228}Th activity was about 30 dpm m^{-3}, this is a minimum estimate considering the low salinity of this particular spring.

The^{224}Ra/^{228}Ra activity ratio in Lake Kinneret is drastically lower than the 1.5 value in the springs. This ratio was measured directly by γ-spectrometry (probably with a considerable error) to be 0.1 at station A (the Kinneret line in Fig. 3, which is the weighted average of surface and bottom samples). Calculation based on separate measurements of ^{224}Ra and ^{228}Ra activities in the lake (not on the same sample) and dividing the extreme values (for both numerator and denominator) yielded a range for the ^{224}Ra/^{228}Ra ratio in Lake Kinneret between 0.0015 and 0.3, well below the ratio of 1.5 for the saline springs. We conclude therefore that within the likelihood of errors, the average ^{224}Ra/^{228}Ra ratio of Lake Kinneret is 0.1. The shaded area around the Kinneret line in Fig. 3 represents the possible variations in the ^{224}Ra/^{228}Ra ratio of Lake Kinneret (e.g., the average surface water ratio is 0.05, deep water ratio is 0.2).

Whereas it is rather clear that the input of the long-lived Ra isotopes is dominated by the saline springs, ^{224}Ra and ^{223}Ra may also enter the lake by diffusion from the sediments and the relative contribution of this source is not known. The role of ^{224}Ra input from those two sources can be estimated by comparing ^{224}Ra and ^{222}Rn activities in the Fuliya saline spring group, the ^{224}Ra in the lake just off the inflow, with ^{224}Ra and ^{222}Rn activities at the surface and bottom of station A (data in Table 1). Whereas ^{224}Ra in the lake bottom water is 16 dpm m^{-3} at the surface it is 5.4 dpm m^{-3}. This suggests input from the bottom which may be interpreted as either input of some kind of a submerged spring, or diffusion from the sediment. The latter explanation is however less likely in view of the ^{222}Rn/^{226}Ra activity ratios that were 3 and 6 for bottom and surface respectively, suggesting that ^{222}Rn enrichment at the surface is larger than near the bottom. Moreover, surface ^{222}Rn activity at station A is larger than its bottom activity, opposite to the expected activities if Rn was supplied from the bottom and lost by gas-exchange at the surface (Table 1). The surface enrichment of ^{222}Rn must therefore stem from input from the saline springs on the shore, in agreement with the very high ^{222}Rn activities at Fuliya (~10,000,000 dpm m^{-3}) and the ^{222}Rn/^{226}Ra activity ratio ranging from 100 to 1300. Since both ^{226}Ra and chlorinity are added to the lake from the springs into the epiliminion (Nishri and Stiller, 1997; Kolodny et al., 1999), we assume that the same holds for the short-lived Ra isotopes as well. Indeed, the ^{224}Ra activity in the surface water off the Fuliya springs is the highest measured within the lake (40 dpm m^{-3}).

The considerable decrease in the ^{224}Ra/^{228}Ra activity ratio in Lake Kinneret stems from preferential adsorption of ^{228}Th (the parent of ^{224}Ra) on suspended particles in the lake upon the saline springs entrance into the freshwater lake. It is most probably adsorbed on bio-detritus, POM and other kinds of particulate matter such as plankton (both phytoplankton and zooplankton) and detrital, airborne and authigenic minerals (such as $CaCO_3$ and $BaSO_4$). This suggestion is corroborated by the finding of Emerson and Hesslein (1973), who have shown that even the less reactive ^{226}Ra is efficiently adsorbed on such material. If the adsorption rate constant for Th were to be the same as the adsorption rate constant for Ra we would expect that the steady state ^{224}Ra/^{228}Ra activity ratio of 1.5 in the springs would also be the ratio of the Kinneret, which is not the case. We make no attempt at the present stage to identify the specific mode of removal of radio-nuclides from the lake. It is very likely that the biomass (as particulate organic matter) and its quantity play a major role it this process (as it did in the experiment of Emerson and Hesslein, 1973). Here it is considered only as "bulk removal".

The ^{223}Ra (a member of the ^{235}U series) enters the lake from the saline springs, and adsorbs onto particles similarly to ^{226}Ra (a member of the ^{238}U series) but decays much faster. The lower ^{224}Ra/^{223}Ra activity ratio in the lake (ca. 4) as compared to that ratio in the saline springs (ca. 8; Table 1) reflects the shorter half life ($T_{1/2} = 3.7$ d) of ^{224}Ra compared to ^{223}Ra ($T_{1/2} = 11.4$ d) while their adsorption rate constants are the same. Obviously, a quantitative estimate of the change in the ^{224}Ra/^{223}Ra ratio from the springs to the lake should also consider the ^{224}Ra produced by the decay of ^{228}Th which by itself is a decay product of the ^{228}Ra dissolved in Lake Kinneret. Similar reasoning applies to the supply of ^{227}Ac (the grandfather of ^{223}Ra), to the lake by the saline springs. We repeatedly measured the activity of the latter during forty days after sampling of Fuliya 2 spring. The activity of ^{223}Ra decreased with an apparent half life of 10 d, which is within experimental error of the "real" ^{223}Ra half life of 11.4 d. We concluded therefore that the supply of ^{227}Ac to the Kinneret by the saline springs is negligible. As will be shown below, ^{224}Ra produced by decay of ^{228}Th is negligible due to the fast disappearance of ^{228}Th from the lake water.

The distinct chemical behavior of the various nuclides in the U–Th decay series, the Ra quartet data and the unique "natural experiment" setting of the Kinneret in which a freshwater lake obtains its Ra from saline springs enabled the development of a simple mass-balance model for the radionuclides in Lake Kinneret. The model is comprised of simultaneous mass balance equations; one for each radionuclide. The equations have one input term: supply of radionuclides from the saline springs; and three output terms: adsorption on particles in the lake, radioactive decay within the lake and outflow from the lake. The model predicts very well the Ra isotopic ratios observed in the lake and yielded estimates of the overall Ra and Th adsorption rate constants in freshwater lakes.

4. THE ^{226}Ra, ^{223}Ra, ^{228}Ra, ^{228}Th AND ^{224}Ra MASS-BALANCE MODEL FOR LAKE KINNERET

The time dependence of all Ra isotopes and ^{228}Th activities in Lake Kinneret can be simulated assuming that ^{226}Ra (^{238}U decay chain) and ^{223}Ra (^{235}U decay chain), ^{228}Ra, ^{228}Th and ^{224}Ra (^{232}Th decay chain) enter the Kinneret only *via* the saline springs. We realize that this assumption is a simplification of the lake system and the calculations should be considered as a first approximation. Nevertheless, additional Ra sources such as diffusive flux from the sediments

and airborne supply are probably small. This is indicated by the total ^{226}Ra flux from saline springs into Lake Kinneret [calculated by multiplying the ^{226}Ra/Cl ratio in the saline springs (Table 1) by the Cl^- annual input into the lake (ca. 10^{11} g Cl^- according to Kolodny et al., 1999)], yielding 62×10^{10} dpm ^{226}Ra y^{-1} which is at least an order of magnitude larger than the world average oceanic flux from sediments for an area equivalent to Lake Kinneret [multiplying 80 atoms ^{226}Ra cm^{-2} min^{-1} according to Broecker and Peng, 1982, p. 204, by the Kinneret area of 168 km^2, yields 5.8×10^{10} dpm ^{226}Ra y^{-1}]. The supply of ^{226}Ra by the Jordan River is negligible (0.012×10^{10} dpm ^{226}Ra $\times$ y^{-1}) compared to the spring input. This is a very conservative estimate considering that the Ra flux from Kinneret sediments comes from fresh porewater (reduced Ra mobility) while the oceanic flux is in saline water (enhanced Ra mobility). The results of our study (see below) show that the above approximation of the ^{226}Ra flux leads to predicted Ra nuclide activities and activity ratios that are very close to the observed ones, suggesting that we did not neglect any significant processes.

Upon entrance to the lake the Ra isotopes mix, decay, adsorb on suspended solids and leave the lake through the National Water Carrier (Fig. 4). The nuclides enter the lake with the saline springs' composition and leave the lake with the Lake's composition. In contrast to the nuclides input by the saline springs, the main water supply to Lake Kinneret, the Jordan River in the north (Figs. 1, 4), adds only a small portion (about 0.2‰, see above) of the relevant nuclides to the lake. According to this model, the governing mass balance equations for ^{226}Ra, ^{223}Ra, ^{228}Ra, in the Kinneret are:

$$\frac{d[^{22i}Ra]_{Kin}}{d[t]} = k_{spg}^{Water} \cdot [^{22i}Ra]_{spg} - k_{22i}^{Ra^*} \cdot [^{22i}Ra]_{Kin} \quad (1)$$

where the digit i denotes 6, 3 and 8 respectively such that $[^{22i}Ra]_{Kin}$ and $[^{22i}Ra]_{spg}$ are the concentrations of the relevant nuclides in Lake Kinneret (subscript Kin) and the saline springs (subscript spg), respectively, in atoms m^{-3}; $k_{spg}^{Water} = \frac{Q_{spg}}{V_{Kin}}$, where V_{Kin} is the volume of Lake Kinneret in m^3 and Q_{spg} is the flux of water from the saline springs to Lake Kinneret in m^3 d^{-1}. The overall output rate coefficient $k_{22i}^{Ra^*}$ is described by the equation:

$$k_{22i}^{Ra^*} = \frac{Q_{Kin,out}}{V_{Kin}} + \lambda_{22i}^{Ra} + k_{W-S}^{Ra}$$

where $Q_{Kin,out}$ is the outflow of water from Lake Kinneret in m^3 d^{-1}; λ_{22i}^{Ra} is the decay constants of the relevant nuclides in d^{-1}; k_{W-S}^{Ra} is the first order "apparent" kinetic constant of adsorption for Ra in d^{-1} including both adsorption and particle settling. Because the rate constants for both Ra and Th (Eq. (2) below) estimated in this study are relatively large, we treat this rate constant as representing pure adsorption.

The mass balance equations for the two daughters of ^{228}Ra, ^{228}Th and ^{224}Ra, are:

$$\frac{d[^{228}Th]_{Kin}}{dt} = k_{spg}^{Water} \cdot [^{228}Th]_{spg} + \lambda_{228}^{Ra} \cdot [^{228}Ra]_{Kin} - k_{228}^{Th^*} \cdot [^{228}Th]_{Kin} \quad (2)$$

$$\frac{d[^{224}Ra]_{Kin}}{dt} = k_{spg}^{Water} \cdot [^{224}Ra]_{spg} + \lambda_{228}^{Th} \cdot [^{228}Th]_{Kin} - k_{224}^{Ra^*} \cdot [^{224}Ra]_{Kin} \quad (3)$$

$$k_{228}^{Th*} = \frac{Q_{Kin,out}}{V_{Kin}} + \lambda_{228}^{Th} + k_{W-S}^{Th}$$

$$k_{224}^{Ra^*} = \frac{Q_{Kin,out}}{V_{Kin}} + \lambda_{224}^{Ra} + k_{W-S}^{Ra}$$

$[^{228}Ra]_{Kin}$,$[^{228}Th]_{Kin}$, $[^{224}Ra]_{Kin}$,$[^{228}Ra]_{spg}$, $[^{228}Th]_{spg}$ and $[^{224}Ra]_{spg}$ are the concentrations of the relevant nuclides in Lake Kinneret (subscript Kin) and the saline springs (sub-

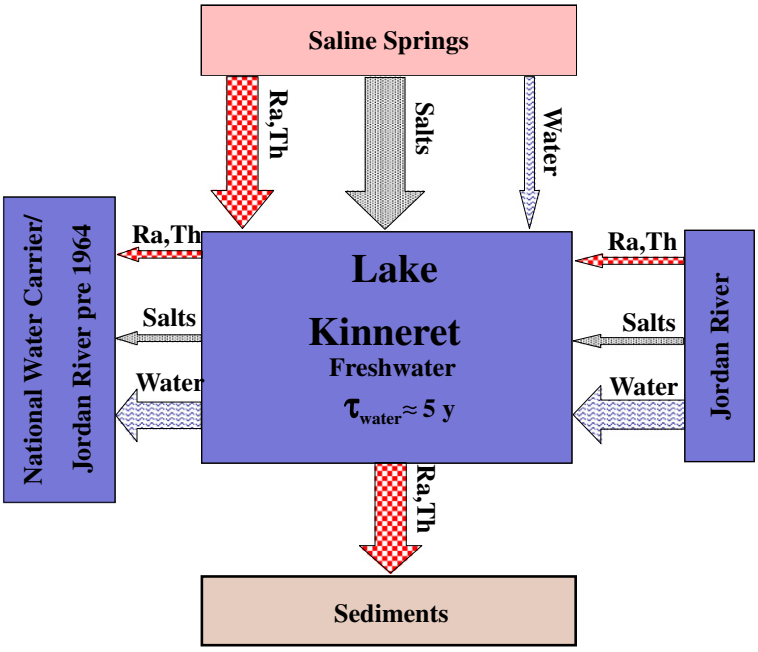

Fig. 4. Schematic box model of Lake Kinneret describing the main inputs and outputs of water, salt as well as Ra and Th nuclides. The sizes of inputs and outputs are represented by the three different types of arrows. Arrow width represents the size of fluxes.

script spg), respectively, in atoms m^{-3}; λ_{228}^{Ra}, λ_{228}^{Th} and λ_{224}^{Ra} are the decay constants of the relevant nuclides in d^{-1}; and k_{W-S}^{Th} is the first order kinetic constant of adsorption for Th in d^{-1}. The notation of the rest is similar to Eq. (1).

The general solution for Eq. (1) describes the activities of all three nuclides (^{223}Ra, ^{226}Ra, ^{228}Ra) in Lake Kinneret as a function of time starting from a hypothetical perturbation that occurred at an arbitrary time defined as $t = 0$.

$$[A^{22i}\mathrm{Ra}]_{\mathrm{Kin}} = \frac{k_{\mathrm{spg}}^{\mathrm{Water}}}{k_{22i}^{\mathrm{Ra}^*}} \cdot [A^{22i}\mathrm{Ra}]_{\mathrm{spg}} \cdot \left(1 - \mathrm{e}^{-k_{22i}^{\mathrm{Ra}^*} \cdot t}\right) + [A^{22i}\mathrm{Ra}]_{\mathrm{Kin},0} \cdot \mathrm{e}^{-k_{22i}^{\mathrm{Ra}^*} \cdot t} \quad (4)$$

where the subscript Kin,0 denotes Lake Kinneret at time zero, and the activities are expressed in dpm m^{-3}.

The solutions for the activities of ^{228}Th and ^{224}Ra are:

$$[\mathrm{A}^{228}\mathrm{Th}]_{\mathrm{Kin}} = \frac{k_{\mathrm{spg}}^{\mathrm{Water}}}{k_{228}^{\mathrm{Th}^*}} \cdot \left(\frac{\lambda_{228}^{\mathrm{Th}}}{k_{228}^{\mathrm{Ra}^*}} \cdot [\mathrm{A}^{228}\mathrm{Ra}]_{\mathrm{spg}} + [\mathrm{A}^{228}\mathrm{Th}]_{\mathrm{spg}}\right) \cdot \left(1 - \mathrm{e}^{-k_{228}^{\mathrm{Th}^*} \cdot t}\right) + \left(\frac{\lambda_{228}^{\mathrm{Th}}}{\left(k_{228}^{\mathrm{Th}^*} - k_{228}^{\mathrm{Ra}^*}\right)} \cdot [\mathrm{A}^{228}\mathrm{Ra}]_{\mathrm{Kin},0} - \frac{\lambda_{228}^{\mathrm{Th}} \cdot k_{\mathrm{spg}}^{\mathrm{Water}}}{k_{228}^{\mathrm{Ra}^*} \cdot \left(k_{228}^{\mathrm{Th}^*} - k_{228}^{\mathrm{Ra}^*}\right)} \cdot [\mathrm{A}^{228}\mathrm{Ra}]_{\mathrm{spg}}\right) \cdot \left(\mathrm{e}^{-k_{228}^{\mathrm{Ra}^*} \cdot t} - \mathrm{e}^{-k_{228}^{\mathrm{Th}^*} \cdot t}\right) + [\mathrm{A}^{228}\mathrm{Th}]_{\mathrm{Kin},0} \cdot \mathrm{e}^{-k_{228}^{\mathrm{Th}^*} \cdot t} \quad (5)$$

$$[\mathrm{A}^{224}\mathrm{Ra}]_{\mathrm{Kin}} = \frac{k_{\mathrm{spg}}^{\mathrm{Water}}}{k_{224}^{\mathrm{Ra}^*}} \cdot \left([\mathrm{A}^{224}\mathrm{Ra}]_{\mathrm{spg}} + \frac{\lambda_{228}^{\mathrm{Th}} \cdot \lambda_{224}^{\mathrm{Ra}}}{k_{228}^{\mathrm{Th}^*} \cdot k_{228}^{\mathrm{Ra}^*}} \cdot [\mathrm{A}^{228}\mathrm{Ra}]_{\mathrm{spg}} + \frac{\lambda_{224}^{\mathrm{Ra}}}{k_{228}^{\mathrm{Th}^*}} \cdot [\mathrm{A}^{228}\mathrm{Th}]_{\mathrm{spg}}\right) \cdot \left(1 - \mathrm{e}^{-k_{224}^{\mathrm{Ra}^*} \cdot t}\right) + \frac{\lambda_{228}^{\mathrm{Th}} \cdot \lambda_{224}^{\mathrm{Ra}}}{\left(k_{224}^{\mathrm{Ra}^*} - k_{228}^{\mathrm{Ra}^*}\right) \cdot \left(k_{228}^{\mathrm{Th}^*} - k_{228}^{\mathrm{Ra}^*}\right)} \cdot \left([\mathrm{A}^{228}\mathrm{Ra}]_{\mathrm{Kin},0} - \frac{k_{\mathrm{spg}}^{\mathrm{Water}}}{k_{228}^{\mathrm{Ra}^*}} \cdot [\mathrm{A}^{228}\mathrm{Ra}]_{\mathrm{spg}}\right) \cdot \left(\mathrm{e}^{-k_{228}^{\mathrm{Ra}^*} \cdot t} - \mathrm{e}^{-k_{224}^{\mathrm{Ra}^*} \cdot t}\right) + \frac{\lambda_{224}^{\mathrm{Ra}}}{\left(k_{224}^{\mathrm{Ra}^*} - k_{228}^{\mathrm{Th}^*}\right)} \cdot \left[\frac{\lambda_{228}^{\mathrm{Th}}}{\left(k_{228}^{\mathrm{Th}^*} - k_{228}^{\mathrm{Ra}^*}\right)} \cdot \left(\frac{k_{\mathrm{spg}}^{\mathrm{Water}}}{k_{228}^{\mathrm{Th}^*}} \cdot [\mathrm{A}^{228}\mathrm{Ra}]_{\mathrm{spg}} - [\mathrm{A}^{228}\mathrm{Ra}]_{\mathrm{Kin},0}\right) + [\mathrm{A}^{228}\mathrm{Th}]_{\mathrm{Kin},0} - \frac{k_{\mathrm{spg}}^{\mathrm{Water}}}{k_{228}^{\mathrm{Th}^*}} \cdot [\mathrm{A}^{228}\mathrm{Th}]_{\mathrm{spg}}\right] \cdot \left(\mathrm{e}^{-k_{228}^{\mathrm{Th}^*} \cdot t} - \mathrm{e}^{-k_{224}^{\mathrm{Ra}^*} \cdot t}\right) + [\mathrm{A}^{224}\mathrm{Ra}]_{\mathrm{Kin},0} \cdot \mathrm{e}^{-k_{224}^{\mathrm{Ra}^*} \cdot t} \quad (6)$$

And the steady state activities of each nuclide are:

$$[\mathrm{A}^{22i}\mathrm{Ra}]_{\mathrm{Kin,SS}} = \frac{k_{\mathrm{spg}}^{\mathrm{Water}}}{k_{22i}^{\mathrm{Ra}^*}} \cdot [\mathrm{A}^{22i}\mathrm{Ra}]_{\mathrm{spg}} \quad (7)$$

$$[\mathrm{A}^{228}\mathrm{Th}]_{\mathrm{Kin,SS}} = \frac{k_{\mathrm{spg}}^{\mathrm{Water}}}{k_{228}^{\mathrm{Th}^*}} \cdot \left(\frac{\lambda_{228}^{\mathrm{Th}}}{k_{228}^{\mathrm{Ra}^*}} \cdot [\mathrm{A}^{228}\mathrm{Ra}]_{\mathrm{spg}} + [\mathrm{A}^{228}\mathrm{Th}]_{\mathrm{spg}}\right) \quad (8)$$

$$[\mathrm{A}^{224}\mathrm{Ra}]_{\mathrm{Kin,SS}} = \frac{k_{\mathrm{spg}}^{\mathrm{Water}}}{k_{224}^{\mathrm{Ra}^*}} \cdot \left([\mathrm{A}^{224}\mathrm{Ra}]_{\mathrm{spg}} + \frac{\lambda_{228}^{\mathrm{Th}} \cdot \lambda_{224}^{\mathrm{Ra}}}{k_{228}^{\mathrm{Th}^*} \cdot k_{228}^{\mathrm{Ra}^*}} \cdot [\mathrm{A}^{228}\mathrm{Ra}]_{\mathrm{spg}} + \frac{\lambda_{224}^{\mathrm{Ra}}}{k_{228}^{\mathrm{Th}^*}} \cdot [\mathrm{A}^{228}\mathrm{Th}]_{\mathrm{spg}}\right) \quad (9)$$

The steady state activity ratios ^{224}Ra/^{228}Ra and ^{224}Ra/^{223}Ra in Lake Kinneret are expressed by the equation:

$$\left[\frac{\mathrm{A}^{224}\mathrm{Ra}}{\mathrm{A}^{22j}\mathrm{Ra}}\right]_{\mathrm{Kin,SS}} = \left(\frac{k_{22j}^{\mathrm{Ra}^*}}{k_{224}^{\mathrm{Ra}^*}} \cdot \left[\frac{\mathrm{A}^{224}\mathrm{Ra}}{\mathrm{A}^{22j}\mathrm{Ra}}\right]_{\mathrm{spg}} + \frac{\lambda_{224}^{\mathrm{Ra}}}{k_{224}^{\mathrm{Ra}^*}} \cdot \frac{k_{22j}^{\mathrm{Ra}^*}}{k_{228}^{\mathrm{Th}^*}} \cdot \left[\frac{\mathrm{A}^{228}\mathrm{Th}}{\mathrm{A}^{22j}\mathrm{Ra}}\right]_{\mathrm{spg}} + \frac{\lambda_{224}^{\mathrm{Ra}}}{k_{224}^{\mathrm{Ra}^*}} \cdot \frac{\lambda_{228}^{\mathrm{Th}}}{k_{228}^{\mathrm{Th}^*}}\right) \quad (10)$$

where the digit j denotes 8 or 3 (representing ^{228}Ra and ^{223}Ra respectively).

It should be noticed that the steady state activity ratios in Lake Kinneret depend only on the proper rate constants (k^* of the Ra isotopes and that of ^{228}Th, all include the outflow rate from Lake Kinneret) and the activity ratios in the saline springs.

Substituting the proper rate constants for the water, saline springs and radioactive decay for a certain initial condition, one can simulate the time behavior of the nuclides for different Ra and Th adsorption rate constants. The set of adsorption constants that yield steady state nuclide ratios of the present Lake Kinneret provides a field based estimate for these constants in freshwater.

5. SIMULATIONS OF THE RADIONUCLIDE ACTIVITIES AND ACTIVITY RATIOS IN LAKE KINNERET

5.1. ^{228}Ra, ^{228}Th and ^{224}Ra and the ^{224}Ra/^{228}Ra ratio

Simulations of the temporal variations of ^{228}Ra, ^{228}Th and ^{224}Ra and of the ^{224}Ra/^{228}Ra ratio (Eqs. (4)–(6) and the quotient of Eq. (6) to Eq. (4)) were conducted using the mass-balance model described above (Fig. 5). The simulation conditions were: $k_{\mathrm{spg}}^{\mathrm{Water}} = 1/60\mathrm{y}^{-1}$ (the saline springs would fill up the lake within 60 y), $Q_{\mathrm{Kin,out}}/V_{\mathrm{Kin}} = 1/5\ \mathrm{y}^{-1}$ (the residence time of water is 5 y). The initial activities of the nuclides in the Kinneret were taken to be their activities in the saline springs diluted to the salinity of Lake Kinneret assuming that in the saline springs the activity of the long lived ^{228}Th is identical to the activity of the short lived ^{224}Ra (secular equilibrium). Four simulations for different Ra adsorption rate constants ($k_{\mathrm{W-S}}^{\mathrm{Ra}}$ =0, 0.01, 0.05, and 0.1 d^{-1}) were conducted in order to investigate the effect of adsorption rate constant on the behavior of the nuclides in Lake Kinneret. The simulations were run assuming that $k_{\mathrm{W-S}}^{\mathrm{Th}} = 100 \cdot k_{\mathrm{W-S}}^{\mathrm{Ra}}$ (where not stated otherwise), meaning that Th adsorbs 100 times faster than Ra. The factor 100 was selected for the test simulations based on the wide information in the literature showing that this is a reasonable ratio between the distribution coefficients of Th and Ra. The range of values for Th distribution coefficients as reported in the literature varies by a factor of 10^5 (10^3 to 10^8) depending on the substrate (see compilation by Santschi et al., 2006), well within the factor used here. Regarding studies dealing with both elements, Allard et al. (1979), quoted in EPA, 1999, 2004 determined experimentally the distribution coefficients K_d for adsorption of Th and Ra from fresh water onto crushed granite. He obtained 100–

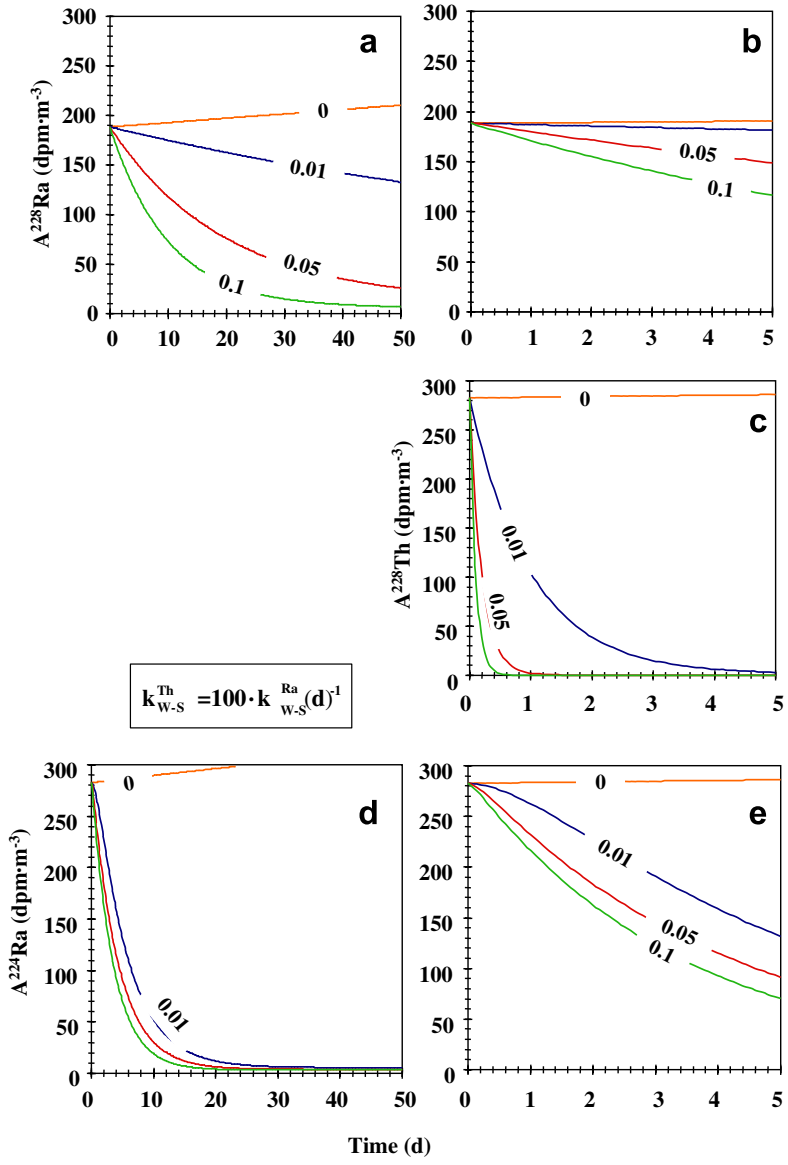

Fig. 5. Simulations (using Eq. (4)–(6)) of the behavior of ^{228}Ra (**a** and **b**), ^{228}Th **(c)** and ^{224}Ra (**d** and **e**) as a function of time for four different adsorption rate constants for Ra ($k^{Ra}_{W-S} = 0, 0.01, 0.05$, and $0.1\ d^{-1}$) assuming that $k^{Th}_{W-S} = 100 \cdot k^{Ra}_{W-S}$. The graphs on the right are blowups of the first 5 days of the graphs on the left. The initial activities for the simulations are the saline springs activities diluted to the salinity of Lake Kinneret assuming that in the saline springs system (spring water + coating on conduits) the activity of the long lived ^{228}Th is identical to the activity of the short lived ^{224}Ra (secular equilibrium). The initial assumed activities of ^{228}Ra, ^{228}Th and ^{224}Ra were 180, 270 and 270 dpm m^{-3}, respectively. Note the lines representing $k^{Ra}_{W-S} = 0\ d^{-1}$ simulating a case in which neither Ra nor Th are adsorbed in the Kinneret. In this case, the nuclides are accumulating in the lake. As shown in Fig. 8 below they reach steady state activities within ca. 6 y. For cases where Ra adsorption is significant ($k^{Ra}_{W-S} > 0$) the nuclides reach steady state within 2 months, in the order ^{228}Th (within several days), ^{224}Ra (within 20 days) and ^{228}Ra (within 2 months).

500 L kg^{-1} for Ra, and 4000–5000 L kg^{-1} for Th. We assume that the ratio between K_d values should be similar to the ratio between the corresponding k (adsorption rate constants) values. Similarly Krest and Harvey (2003) quoted K_d (dimensionless) for Th as 10^4–10^5 and for Ra as 10^2–10^3, consistent with a ratio of 100 we used.

The simulations reveal that when k^{Ra}_{W-S} is 0.05 d^{-1} ^{228}Ra decreases by almost an order of magnitude in 50 d and ^{228}Th is almost totally depleted within 1 d (Fig. 5 a-c). The effect of the value of k^{Ra}_{W-S} (and k^{Th}_{W-S}) on ^{224}Ra is rather small and already at $k^{Ra}_{W-S} = 0.01\ d^{-1}$ ^{224}Ra decreases by an order of magnitude within 20 d (Fig. 5d, e). Without adsorption, the activity of all nuclides in the lake would be considerably higher (the lines representing $k^{Ra}_{W-S} = 0\ d^{-1}$ in Fig. 5). For cases where Ra adsorption is significant ($k^{Ra}_{W-S} > 0$) the nuclides reach steady state within 2 months, in the order ^{228}Th (within several days), ^{224}Ra (within 20 days) and ^{228}Ra (within 2 months). The behavior of the three nuclides indicates that in order to decrease the ^{224}Ra/^{228}Ra activity ratio from its rather high initial ratio

of 1.5 to the low 0.1 ratio in the Kinneret (Fig. 3, Table 1) the k^{Ra}_{W-S} should be lower than 0.05 d^{-1} and close to 0.01 d^{-1}. This is best demonstrated when plotting the $^{224}Ra/^{228}Ra$ activity ratios versus time for different k^{Ra}_{W-S} (Fig. 6). Using any of the k^{Ra}_{W-S} values the $^{224}Ra/^{228}Ra$ ratios go through a minimum but for their steady state values the ratios depend on the k^{Ra}_{W-S} value. When $k^{Ra}_{W-S} = 0.01$ d^{-1}, the steady state $^{224}Ra/^{228}Ra$ activity ratio is within the range of the observed $^{224}Ra/^{228}Ra$ activity ratios of Lake Kinneret (shaded area in Fig. 6).

Plotting the variations of the steady state $^{224}Ra/^{228}Ra$ activity ratio (Eq. (10)) versus Ra adsorption rate constant (k^{Ra}_{W-S}) enable constraining the range of $k^{Th}_{W-S}/k^{Ra}_{W-S}$ ratio for the lake (Fig. 7). The plot shows that in order to simulate the $^{228}Ra/^{224}Ra$ activity ratio of the Kinneret k^{Ra}_{W-S} must be larger than 0.002 d^{-1} but less than 0.02 d^{-1} and $k^{Th}_{W-S}/k^{Ra}_{W-S}$ must be larger than 50. As mentioned above and as shown in Fig. 8, it is not possible to simulate either the nuclides activities or the $^{224}Ra/^{228}Ra$ activity ratio of Lake Kinneret without proposing the adsorption of the nuclides on particles when the saline springs enter the lake

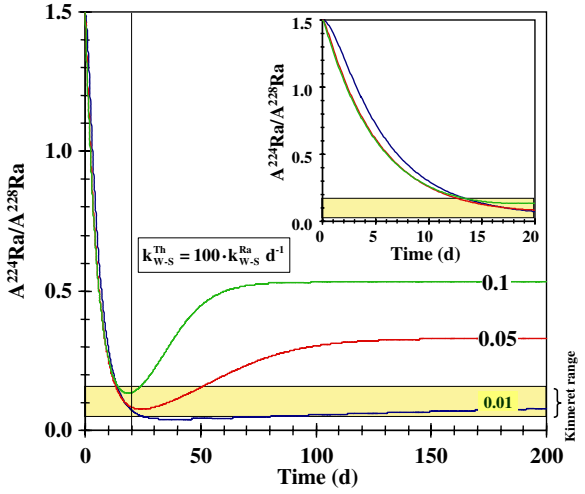

Fig. 6. Simulations of the behavior of the $^{224}Ra/^{228}Ra$ activity ratio (Eq. (6) divided by Eq. (4)) as a function of time for three different adsorption rate constants for Ra ($k^{Ra}_{W-S} = 0.01$, 0.05, and 0.1 d^{-1}) assuming $k^{Th}_{W-S} = 100 \cdot k^{Ra}_{W-S}$. The insert is a blowup of the first 20 days. The initial activity ratio for the simulations was taken as the $^{228}Ra/^{224}Ra$ activity ratio of the saline springs (1.5, see Fig. 3). Note that even though all three lines reach the activity ratio range of the Kinneret (shaded area) within ca. 20 d (see insert), only the line of the lowest rate constant ($k^{Ra}_{W-S} = 0.01$) stays in the Kinneret range at steady state. At this rate constant, $k^{Ra^*}_{224} \gg k^{Ra^*}_{228}$, $k^{Ra^*}_{228}$ is determined only by k^{Ra}_{W-S} (because $k^{Ra}_{W-S} \gg \lambda^{Ra}_{228}$), $k^{Ra^*}_{224}$ is determined by decay (because $\lambda^{Ra}_{224} \sim 0.2 d^{-1} \gg k^{Ra}_{W-S}$) and the $^{224}Ra/^{228}Ra$ activity ratio decreases fast in ca. 20 d and then increases very slowly towards a steady state value that is about $1.2 \cdot \frac{k^{Ra^*}_{228}}{k^{Ra^*}_{224}} \cdot \left[\frac{A^{224}Ra}{A^{22}/Ra}\right]_{spg}$ (see Eq. (11)). The value of $\frac{k^{Ra^*}_{228}}{k^{Ra^*}_{224}}$ at this stage is smaller then unity. When k^{Ra}_{W-S} increases and becomes 25% of λ^{Ra}_{224}, $k^{Ra^*}_{224}$ grows significantly above λ^{Ra}_{224} while $k^{Ra^*}_{228}$ grows exactly as k^{Ra}_{W-S}. At this stage $\frac{k^{Ra^*}_{228}}{k^{Ra^*}_{224}}$ becomes considerably larger then unity and the steady state $^{224}Ra/^{228}Ra$ activity ratio increases considerably after reaching the minimum.

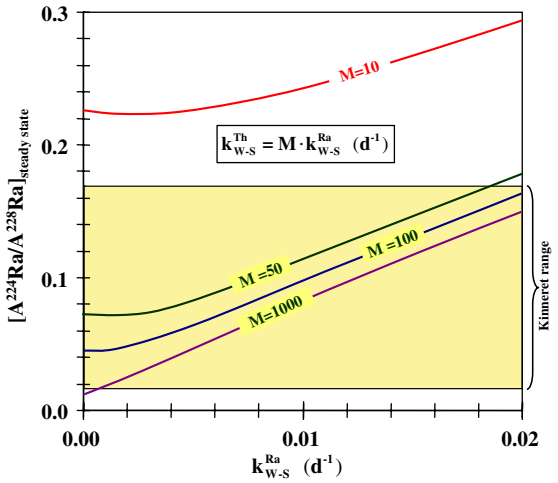

Fig. 7. Simulations of the steady state $^{224}Ra/^{228}Ra$ activity ratio (Eq. (10)) as a function of the Ra adsorption rate constant for different ratios of Th to Ra adsorption rate constants ($k^{Th}_{W-S}/k^{Ra}_{W-S} = 10$, 50, 100 and 1000). For $k^{Ra}_{W-S} < 0.002$ d^{-1} the k^{Th}_{W-S} were forced to remain unchanged and only the k^{Ra}_{W-S} is decreasing. Without this forcing the steady state $^{228}Ra/^{224}Ra$ activity ratio would increase considerably when the adsorption rate constant of Ra approaches zero. The plot indicates that in order to stay in the range of $^{224}Ra/^{228}Ra$ activity ratio of the Kinneret (the shaded area) k^{Ra}_{W-S} should be between 0.002 and 0.02 d^{-1} and the $k^{Th}_{W-S}/k^{Ra}_{W-S}$ ratio should exceed 50.

(Fig. 8). It should be noted that unlike for the case with adsorption (Fig. 6) where steady state of the $^{224}Ra/^{228}Ra$ activity ratio is achieved within days, the activity ratio of 1.5 for "no adsorption" is achieved within ca. 6 y. In addition, this steady state ratio is much higher then the observed Kinneret value (shaded area).

In order to corroborate the values of the rate constants for Ra and Th estimated from the members of the ^{232}Th decay series, we add in the next section simulations of ^{223}Ra and ^{226}Ra (Eq. (4)), which are members of ^{235}U and ^{238}U decay series, respectively. Simulating the behavior of these nuclides using the same rate constants will add the redundancy needed to check the validity of the estimates.

5.2. ^{226}Ra activity and the $^{224}Ra/^{223}Ra$ activity ratio

A plot of $^{224}Ra/^{228}Ra$ and $^{224}Ra/^{223}Ra$ activity ratios as a function of time (Fig. 9, division of Eq. (6) by Eq. (4)) shows that the simulation yields at steady state the observed $^{224}Ra/^{228}Ra$ and $^{224}Ra/^{223}Ra$ activity ratios of Lake Kinneret. The steady state is achieved within about 1 and 3 months for $^{224}Ra/^{228}Ra$ and $^{224}Ra/^{223}Ra$, respectively (the shaded areas in Fig. 9, the activity ratios in Lake Kinneret). The steady state for $^{224}Ra/^{228}Ra$ activity ratio was achieved sooner than the steady state for the $^{224}Ra/^{223}Ra$ activity ratio due to the large difference in the decay constants of ^{224}Ra and ^{228}Ra and the similarity in the decay constants of ^{224}Ra and ^{223}Ra. Whereas the decay constant for ^{223}Ra is smaller than for ^{224}Ra, ^{228}Ra behaves as a stable element over the timescale examined. Simulation of the behavior of the long lived ^{226}Ra (Eq. (4)) shows that adsorption only, is

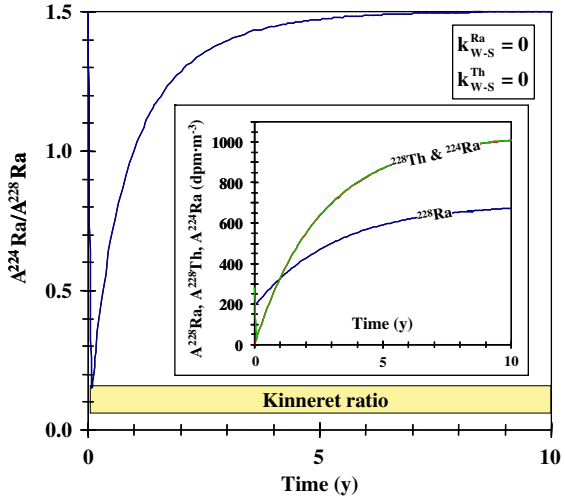

Fig. 8. Simulation of the ^{224}Ra/^{228}Ra activity ratio in Lake Kinneret as a function of time assuming no adsorption ($k^{Th}_{W-S} = k^{Ra}_{W-S} = 0$), the simulated activities of ^{228}Ra, ^{228}Th, ^{224}Ra are shown in the insert. Note that unlike for the case with adsorption (Fig. 6) where steady state of the ^{224}Ra/^{228}Ra activity ratio is achieved within days, the activity ratio of 1.5 for "no adsorption" is achieved within ca. 6 y. In addition, this steady state ratio is much higher then the observed Kinneret value (shaded area).

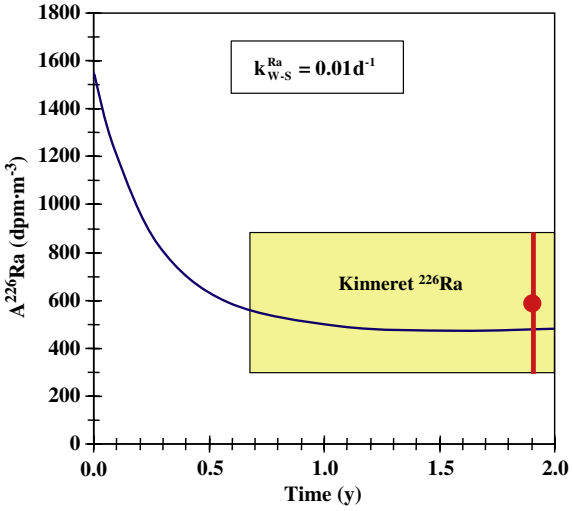

Fig. 10. Simulation of the ^{226}Ra activity in Lake Kinneret as a function of time (Eq. (4)) assuming initial activity of Fuliya group springs diluted to Lake Kinneret salinity (1700 dpm m^{-3}), $k^{Ra}_{W-S} = 0.01$ d^{-1}. The ^{226}Ra reaches the Kinneret value in less then a year as represented by the shaded area (^{226}Ra activity of Lake Kinneret) that starts from the time the ^{226}Ra simulated activity reached ca. 0.9 of the ^{226}Ra steady state value.

sufficient to produce a steady-state activity value similar to that of the Kinneret within less than 1 y (Fig. 10). It is possible to estimate k^{Ra}_{W-S} directly from Eq. (7) (independently of all other nuclides) assuming that ^{226}Ra reached steady state. Given the large uncertainty in the ^{226}Ra of the Lake (600 ± 300 dpm m^{-3}) and its variability in the spring system (see Table 1) we calculated adsorption constants ranging from 0.002 to 0.02 d^{-1}. The values we estimated from the simulations above are in the middle of this range.

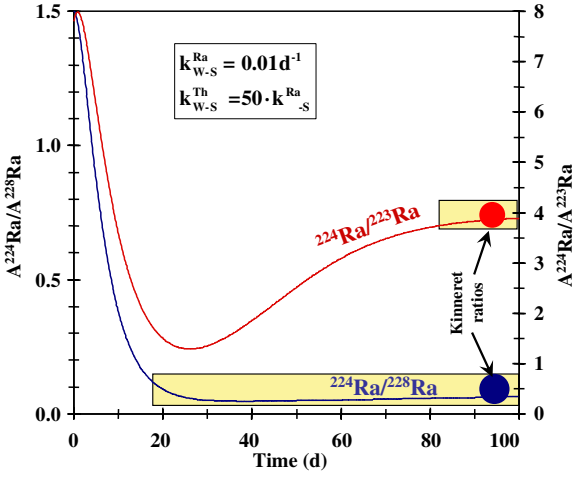

Fig. 9. Simulations of ^{224}Ra/^{228}Ra and ^{224}Ra/^{223}Ra activity ratios (dividing Eq. (6) by Eq. (4); when Eq. (4) represents either ^{223}Ra or ^{228}Ra) as a function of time assuming $k^{Ra}_{W-S} = 0.01$ d^{-1} and $k^{Th}_{W-S} = 50 \cdot K_{Ra}$. Both ratios reach Lake Kinneret values within about 1 and 3 months for ^{224}Ra/^{228}Ra and ^{224}Ra/^{223}Ra, respectively as represented by the shaded areas (the activity ratios in Lake Kinneret) that start from the time the ratios reached ca. 0.95 of the steady state value.

The simulation results of all four Ra nuclides yield the same range of adsorption rate constants: $k^{Ra}_{W-S} \approx 0.005$ to 0.02 d^{-1} and $k^{Th}_{W-S}/k^{Ra}_{W-S} \approx 50$ to 100 ($k^{Th}_{W-S} \approx 0.5$ to 1 d^{-1}). We suggest therefore that these are the adsorption rate constants for "average Lake Kinneret particulate matter" in freshwater. The range k^{Ra}_{W-S} for Lake Kinneret is significantly lower than the constant for Lake 227 (3 d^{-1}, Emerson and Hesslein, 1973 and see "Section 1" above).

5.3. The steady state ^{224}Ra/^{228}Ra and ^{224}Ra/^{223}Ra activity ratios and the residence time of the nuclides in Lake Kinneret

As mentioned above, the steady state ^{224}Ra/^{228}Ra or ^{224}Ra/^{223}Ra activity ratios represented by Eq. (10) do not depend on the water flow from the saline springs. This characteristic increases the confidence in the values of the adsorption rates constants estimated in our study because the total water flow of the monitored and unmonitored saline springs (required for calculating individual nuclide activities by Eqs. (4)–(9)) is poorly known (Kolodny et al., 1999). Assuming that in the saline springs $A\,^{228}\mathrm{Th} = A\,^{224}\mathrm{Ra}$ (as it should be if the $[A\,^{224}\mathrm{Ra}/A\,^{228}\mathrm{Ra}]_{spg} = 1.5$ represents transient equilibrium) the steady state activity ratios can be expressed in a degenerated form of Eq. (10):

$$\left[\frac{A^{224}Ra}{A^{22j}Ra}\right]_{Kin,SS} = \frac{k^{Ra^*}_{22j}}{k^{Ra^*}_{224}} \cdot \left(1 + \frac{\lambda^{Ra}_{224}}{k^{Th^*}_{228}}\right) \cdot \left[\frac{A^{224}Ra}{A^{22j}Ra}\right]_{spg} + \frac{\lambda^{Ra}_{224}}{k^{Ra^*}_{224}} \cdot \frac{\lambda^{Th}_{228}}{k^{Th^*}_{228}} \quad (11)$$

where j denotes 8 or 3.

The steady state activities of each nuclide (Eqs. (7)–(9)) enable calculating the residence time, τ, of the nuclides in Lake Kinneret as follows:

The residence times of ^{226}Ra, ^{228}Ra and ^{223}Ra:

$$\tau_{\mathrm{Ra-22i}} = \frac{V_{\mathrm{Kin}} \cdot [\mathrm{A}^{22i}\mathrm{Ra}]_{\mathrm{Kin,SS}}}{Q_{\mathrm{spg}} \cdot [\mathrm{A}^{22i}\mathrm{Ra}]_{\mathrm{spg}}} = \frac{V_{\mathrm{Kin}} \cdot \frac{k_{\mathrm{spg}}^{\mathrm{Water}}}{k_{22i}^{\mathrm{Ra}^*}} \cdot [\mathrm{A}^{22i}\mathrm{Ra}]_{\mathrm{spg}}}{Q_{\mathrm{spg}} \cdot [\mathrm{A}^{22i}\mathrm{Ra}]_{\mathrm{spg}}} = \frac{1}{k_{22i}^{\mathrm{Ra}^*}} \quad (12)$$

where i denotes 6, 8, 3. The residence times for ^{228}Th and ^{224}Ra:

$$\tau_{\mathrm{Th-228}} = \frac{1}{k_{228}^{\mathrm{Th}^*}} \cdot \left(1 + \frac{\lambda_{228}^{\mathrm{Th}}}{k_{228}^{\mathrm{Ra}^*}} \cdot \frac{[\mathrm{A}^{228}\mathrm{Ra}]_{\mathrm{spg}}}{[\mathrm{A}^{228}\mathrm{Th}]_{\mathrm{spg}}}\right) \quad (13)$$

$$\tau_{\mathrm{Ra-224}} = \frac{1}{k_{224}^{\mathrm{Ra}^*}} \cdot \left(1 + \frac{\lambda_{228}^{\mathrm{Th}} \cdot \lambda_{224}^{\mathrm{Ra}}}{k_{228}^{\mathrm{Th}^*} \cdot k_{228}^{\mathrm{Ra}^*}} \cdot \frac{[\mathrm{A}^{228}\mathrm{Ra}]_{\mathrm{spg}}}{[\mathrm{A}^{224}\mathrm{Ra}]_{\mathrm{spg}}} + \frac{\lambda_{224}^{\mathrm{Ra}}}{k_{228}^{\mathrm{Th}^*}} \cdot \frac{[\mathrm{A}^{228}\mathrm{Th}]_{\mathrm{spg}}}{[\mathrm{A}^{224}\mathrm{Ra}]_{\mathrm{spg}}}\right) \quad (14)$$

assuming that in the saline springs $A\ ^{228}\mathrm{Th} = A\ ^{224}\mathrm{Ra}$ (see above) Eqs. (13) and (14) become:

$$\tau_{\mathrm{Th-228}} = \frac{1}{k_{228}^{\mathrm{Th}^*}} \cdot \left(1 + \frac{\lambda_{228}^{\mathrm{Th}}}{k_{228}^{\mathrm{Ra}^*}} \cdot \frac{[\mathrm{A}^{228}\mathrm{Ra}]_{\mathrm{spg}}}{[\mathrm{A}^{224}\mathrm{Ra}]_{\mathrm{spg}}}\right) \quad (15)$$

$$\tau_{\mathrm{Ra-224}} = \frac{1}{k_{224}^{\mathrm{Ra}^*}} \cdot \left(1 + \frac{\lambda_{224}^{\mathrm{Ra}}}{k_{228}^{\mathrm{Th}^*}} + \frac{\lambda_{228}^{\mathrm{Th}} \cdot \lambda_{224}^{\mathrm{Ra}}}{k_{228}^{\mathrm{Th}^*} \cdot k_{228}^{\mathrm{Ra}^*}} \cdot \frac{[\mathrm{A}^{228}\mathrm{Ra}]_{\mathrm{spg}}}{[\mathrm{A}^{224}\mathrm{Ra}]_{\mathrm{spg}}}\right) \quad (16)$$

The above equations (Eqs. (15) and (16)) yield residence times for ^{226}Ra, ^{228}Ra,^{223}Ra, ^{224}Ra, and ^{228}Th of about 95, 92, 14, 6 and 1 d, respectively. The most reactive element, Th, has the shortest residence time even though its $T_{1/2}$ is 1.9 y. Apparently, its residence time is controlled entirely by its adsorption ($\tau_{\mathrm{Th}} \approx 1/k_{\mathrm{W-S}}^{\mathrm{Th}}$). Among the Ra isotopes, the long lived have longer residence time with no significant difference between ^{226}Ra and ^{228}Ra even though ^{226}Ra has a much longer half life. The residence time of these nuclides is also controlled mainly by adsorption ($\tau_{\mathrm{Ra-226,228}} \approx 0.9 \cdot (1/k_{\mathrm{W-S}}^{\mathrm{Ra}})$). While the residence of the long lived Ra nuclides is determined by their reactivity to be ca. 90 d, the residence time of the short lived Ra nuclides is determined primarily by their decay constant ($\tau_{\mathrm{Ra-224}} \approx 1/\lambda_{224}^{\mathrm{Ra}}$, $\tau_{\mathrm{Ra-223}} \approx 1/\lambda_{223}^{\mathrm{Ra}}$). One consequence of the short residence times of the short-lived Ra isotopes should be offshore lateral gradients of their activities, especially close to the input source.

6. ESTIMATING THE DESORPTION RATE CONSTANT FOR Ra IN LAKE KINNERET

The adsorption rate constants for Lake Kinneret water were estimated in this study as $k_{\mathrm{W-S}}^{\mathrm{Ra}} \approx 0.005$ to $0.02\ \mathrm{d}^{-1}$ and $k_{\mathrm{W-S}}^{\mathrm{Th}} \approx 0.5$ to $1\ \mathrm{d}^{-1}$. These estimates are well within the huge spread (several orders of magnitude) of published adsorption rate constants and distribution coefficients for these elements (e.g., Bacon and Anderson, 1982; Krishnaswami et al., 1982; EPA, 1999, 2004). We therefore consider our estimates as operative rate constants suitable for calculating the fate of Ra and Th in lakes.

The ratio $k_{\mathrm{W-S}}^{\mathrm{Ra}}/k_{\mathrm{S-W}}^{\mathrm{Ra}} = \mathrm{K}'_{\mathrm{Ra}}$ is the definition of the dimensionless equilibrium distribution coefficient of Ra, where $k_{\mathrm{S-W}}^{\mathrm{Ra}}$ is the desorption rate constant in d^{-1} units. Thus, knowing the value of $\mathrm{K}'_{\mathrm{Ra}}$ in Lake Kinneret, $k_{\mathrm{S-W}}^{\mathrm{Ra}}$ can be estimated. The available literature data (Stiller and Imboden, 1986; Kirchner et al., 1997) enable calculating the $K_{\mathrm{D,Ra}}$ that is the equilibrium distribution coefficient in $\mathrm{L\ kg}^{-1}$ in Lake Kinneret. The relationship between these two distribution coefficients is given by the equation:

$$\mathrm{K}'_{\mathrm{Ra}} = \mathrm{K}_{\mathrm{D,Ra}}(\mathrm{L}_{\mathrm{solution}} \cdot \mathrm{kg}_{\mathrm{solid}}^{-1}) \cdot \mathrm{S}(\mathrm{kg}_{\mathrm{solid}} \cdot \mathrm{L}_{\mathrm{solution}}^{-1}) = \left([\mathrm{A}^{226}\mathrm{Ra}]_{\mathrm{solid}}/[\mathrm{A}^{226}\mathrm{Ra}]_{\mathrm{liquid}}\right) \cdot S$$

where S is the suspended load in the Kinneret. The ^{226}Ra activity in Kinneret bottom sediments is about 2500 $\mathrm{dpm\ kg}^{-1}$ (Stiller and Imboden, 1986; Kirchner et al., 1997) of which the unsupported ^{226}Ra (the ^{226}Ra excess over ^{238}U) is 1300 $\mathrm{dpm\ kg}^{-1}$ (based on the average ^{238}U concentration in Kinneret sediments, 1.5 ppm, according to Kronfeld and Stiller, 1997); the activity of dissolved ^{226}Ra in the Kinneret is about 0.6 $\mathrm{dpm\ L}^{-1}$ (average of Stiller and Imboden, 1986 and Table 1); and the suspended load is ca. 3.5×10^{-6} $\mathrm{kg\ L}^{-1}$ (Zohary, 2004). These values yield $\mathrm{K}'_{\mathrm{Ra}}$ of 0.01 when using the unsupported ^{226}Ra and an upper limit of 0.02 when using for calculation the total ^{226}Ra in the sediments. This means that the Ra desorption rate coefficient ($k_{\mathrm{S-W}}^{\mathrm{Ra}}$) is 50–100 times larger than the Ra adsorption rate constant ($k_{\mathrm{W-S}}^{\mathrm{Ra}}$) or that $k_{\mathrm{S-W}}^{\mathrm{Ra}} \approx 0.5$ to $1\ \mathrm{d}^{-1}$. Indeed, desorption rate constants are usually much larger then the adsorption rate constants for elements like Ra (e.g., Krishnaswami et al., 1982).

We did not attempt to estimate the Th desorption rate constant because measurements of dissolved Th in Lake Kinneret are currently not available and using our model estimates of ^{228}Th activities is too speculative for this purpose.

7. SUMMARY

A simple mass-balance model for the Ra isotopes was developed for the unique "natural experiment" conditions in Lake Kinneret, in which saline springs supply radionuclides into a freshwater lake. The model constrains narrowly the Ra and Th adsorption characteristics by tuning the activity ratios of the Ra "quartet" to the observed values in the lake. Specifically, fitting the observed decrease of $^{226}\mathrm{Ra/Cl}^-$ ratio from a range of 6–13 $\mathrm{dpm\ g}^{-1}$ in the springs to about 2 $\mathrm{dpm\ g}^{-1}$ in the lake, as well as the reduction of activity ratios of $^{224}\mathrm{Ra}/^{228}\mathrm{Ra}$, and $^{224}\mathrm{Ra}/^{223}\mathrm{Ra}$ correspondingly from ratios of 1.5 and 8 in the springs to about 0.1 and 4 in the lake, yielded the following rate constants: Ra adsorbed unto particles with a rate between 0.5% and 2% per day and Th is adsorbed at a fifty to a hundred times higher rate of 50–100% per day ($k_{\mathrm{W-S}}^{\mathrm{Ra}} \approx 0.005$ to $0.02\ \mathrm{d}^{-1}$ and $k_{\mathrm{W-S}}^{\mathrm{Th}} \approx 0.5$ to $1\ \mathrm{d}^{-1}$). The Ra desorption rate coefficient was estimated to be 50–100 times larger than its adsorption rate constant. The model shows that radionuclides reach steady state after a rather short time and the observed activity ratios of the Ra nuclides in the lake are all steady state ratios. They depend only on the rate constants

and the activity ratios in the saline springs, and are independent of the flow rate of the saline springs.

ACKNOWLEDGMENTS

We are grateful to Dr. Ami Nishri and the staff of the Israel Oceanographic and Limnological Research Ltd., Yigal Alon Kinneret Limnological Laboratory; Dr. Benjamin Teltsch and the staff of the Lake Kinneret Watershed Unit, Mekorot Water Co.; Dr. Doron Markel the Kinneret coordinator in The Israel Water and Sewage Authority; and Mr. Yossi Sherer of the Institute of Earth Sciences, HU for their help in boat operating, sampling and providing laboratory space. The Moshe Shilo Minerva Center for Marine Biogeochemistry for providing travel budget (B.L.). Dr. Naama Gazit-Yaari generously helped with the γ-spectrometry analyses and Mr. Yehuda Shalem performed the Rn analyses. We benefited from the comments and criticism of the participants of the IAEA "RaDeCC Workshop", Monaco, October 2006 and three anonymous reviewers that substantially improved the manuscript.

REFERENCES

Allard B., Rydberg J., Kipatsi H. and Tornstenfelt B. (1979) Disposal of Radioactive Waste in Granitic Bedrock. In *Radioactive Waste in Geologic Storage, ACS Symposium Series 100* (ed. S. Fried). American Chemical Society, Washington, D.C., pp. 47–73.

Bacon M. P. and Anderson R. F. (1982) Distribution of thorium isotopes between dissolved and particulate forms in the deep sea. *J. Geophys. Res.* **87**, 2045–2056.

Bar-Giora Magal E. (2000) Characterization and location of internal salinity sources in Lake Kinneret, M.Sc. thesis. The Hebrew University of Jerusalem. (Hebrew, English abstract).

Broecker W. S. and Peng T.-H. (1982) *Tracers in the Sea*. Eldigio Press, NewYork, 690 pp.

Chase Z., Anderson R. F., Fleisher M. Q. and Kubik P. W. (2002) The influence of particle composition and particle flux on scavenging of Th, Pa, and Be in the ocean. *Earth Planet. Sci. Lett.* **2004**, 215–229.

Curie P. and Laborde A. (1903) Sur la chaleur de'gage'e spontane'ment par les sels de radium. Comptes rendus de l'Acade'mie des Sciences 136, 673–675. (Translated, On the heat spontaneously released by the salts of radium). In *The Discovery of Radioactivity and Transmutation* (1964) (ed. A. Romer), Dover, New York, pp. 167–169.

Emerson S. and Hesslein R. (1973) Distribution and uptake of artificially introduced Radium-226 in a Small Lake. *J. Fish. Res. Board Canada* **30**, 1485–1490.

Davidson M. R. and Dickson B. L. (1986) A porous flow model for steady state transport of radium in groundwater. *Water Resources Res.* **22**(1), 34–44.

EPA (US Environmental Protection Agency (1999) Understanding Variation in Partition Coefficient, Kd, Values; vol. II: Review of Geochemistry and Available Kd values for Cadmium, Cesium, Chromium, Lead, Plutonium, Radon, Strontium, Thorium, Tritium and Uranium. [EPA 402-R-99-004B.] http://www.epa.gov/radiation/cleanup/partition.htm).

EPA (US Environmental Protection Agency (2004) Understanding Variation in Partition Coefficient, Kd, Values; Volume III—Review of Geochemistry and Available Kd Values for Americium, Arsenic, Curium, Iodine, Neptunium, Radium, and Technetium [EPA 402-R-99-004C], http://www.epa.gov/radiation/cleanup/partition.htm).

Evans R. D. (1955) *The Atomic Nucleus*. McGraw-Hill, 972 pp.

Honeyman B. D., Balistieri L. S. and Murray J. W. (1988) Oceanic trace metal scavenging: the importance of particle concentration. *Deep Sea Res.* **35**, 227–246.

Kirchner G., Stiller M., Nishri A. and Koren N. (1997) A simultaneous measurement of ^{137}Cs, ^{210}Pb and ^{226}Ra in sediments of the Dead Sea and Lake Kinneret by gamma spectrometry. In *The 13th GIF meeting on The Dead Sea Rift as a unique global site*. Terra Nostra—Schriften der Alfred Wegener Stiftung 4/97.

Koczy F. F. (1958) Natural Radium as a tracer in the ocean. *U.N. Int. Conf. Peaceful uses of Atomic Energy*, 351.

Kolodny Y., Katz A., Starinsky A., Simon E. and Moise T. (1999) Chemical tracing of salinity sources in Lake Kinneret (Sea of Galilee), Israel. *Limnol. Oceanogr.* **44**, 1035–1044.

Kraemer T. F. (2005) Radium isotopes in Cayuga Lake, New York: indicators of inflow and mixing processes. *Limnol. Oceanogr.* **50**, 158–168.

Krest J. M. and Harvey J. W. (2003) Using natural distributions of short-lived radium isotopes to quantify groundwater discharge and recharge. *Limnol. Oceanogr.* **48**, 290–298.

Krishnaswami S., Graustein W. C. and Turekian K. K. (1982) Radium thorium and radioactive lead isotopes in groundwaters: application to the in situ determination of adsorption–desorption rate constants and retardation factors. *Water Resources Res.* **18**, 1633–1675.

Krishnaswami S., Bhushan R. and Baskaran M. (1991) Radium isotopes and ^{222}Rn in shallow brines, Kharaghoda (India). *Chem. Geol. (Isot. Geosci. Section)* **87**, 125–136.

Kronfeld J. and Stiller M. (1997) The fate of uranium in the three lakes of the Jordan Rift Valley. *Isr. J. Earth Sci.* **46**, 13–28.

Luo S. and Ku T. L. (1999) Oceanic ^{231}Pa/^{230}Th ratio influenced by particle composition and remineralization. *Earth Planet. Sci. Lett.* **167**, 183–195.

Mathieu G. G., Biscaye P. E., Lupton R. A. and Hammond D. E. (1988) System for measurement of ^{222}Rn at low levels in natural waters. *Health Phys.* **55**, 989–992.

Mazor E. (1962) Radon and radium content of some Israeli water sources and a hypothesis on underground reservoirs of brines, oils and gases in the Rift Valley. *Geochim. Cosmochim. Acta* **26**, 765–786.

Moise T., Starinsky A., Katz A. and Kolodny Y. (2000) Ra isotopes and Rn in brines and ground waters of the Jordan-Dead Sea Rift Valley: enrichment, retardation, and mixing. *Geochim. Cosmochim. Acta.* **64**, 2371–2388.

Moore W. S., Key R. M. and Sarmiento J. L. (1985) Techniques for precise mapping of ^{226}Ra and ^{228}Ra in the ocean. *J. Geophys. Res.* **90**, 6983–6994.

Moore W. S. (1992) Radionuclides of the uranium and thorium decay series in the estuarine environment. In *Uranium-series Disequilibrium: Applications to Earth, Marine, and Environmental Sciences* (eds. M. Ivanovich and R. S. Harmon). Oxford Science publications, Clarendon Press, Oxford, p. 910.

Moore W. S. (1996) Large groundwater inputs to coastal waters revealed by ^{226}Ra enrichments. *Nature* **380**, 612–614.

Moore W. S. (1999) The subterranean estuary: a reaction zone of ground water and sea water. *Marine Chem.* **65**, 111–126.

Moore W. S. and Arnold R. (1996) Measurement of ^{223}Ra and ^{224}Ra in coastal waters using a delayed coincidence counter. *J. Geophys. Res.* **101**, 1321–1329.

Nishri A. and Stiller M. (1997). Radium and Radon measurements in Lake Kinneret. Ministry of National Infrastructure, Report no. T25/97, Israel Oceanographic and Limnological, Research, The Yigal Allon Kinneret Limnological Laboratory.

Nishri A., Stiller M., Rimmer A., Geifman Y. and Krom M. (1999) Lake Kinneret (The Sea of Galilee): the effects of diversion of

external salinity sources, and the probable chemical composition of the internal salinity sources. *Chem. Geol.* **158**, 37–52.

Rama and Moore W. S. (1996) Using the radium quartet for evaluating groundwater input and water exchange in salt marshes. *Geochim. Cosmochim. Acta* **60**, 4645–4652.

Roy-Barman R., Coppola L. and Souhaut M. (2002) Thorium isotopes in the western Mediterranean Sea: an insight into marine particle dynamics. *Earth and Planet. Sci. Lett.* **196**, 161–174.

Santschi P. H., Murray J. W., Baskaran M., Benitez-Nelson C. R., Guo L. D., Hung C.-C., Lamborg C., Moran S. B., Passow U. and Roy-Barman R. (2006) Thorium speciation in seawater. *Marine Chem.* **100**, 250–268.

Stiller M. and Imboden D. M. (1986) ^{210}Pb in Lake Kinneret waters and sediments: residence times and fluxes. In *Sediment and Water Interactions* (ed. P. G. Sly). Springer-Verlag, New York, pp. 501–511.

Waples J. T., Orlandini K. A., Edgington D. N. and Klump J. V. (2004) Seasonal and spatial dynamics of ^{234}Th/^{238}U disequilibria in southern Lake Michigan. *J. Geophys. Res.* **109**, C10S06. doi:10.1029/2003JC002204.

Waples J. T., Benitez-Nelson C., Savoye N., Rutgers van der Loeff M. and Baskaran M. (2006) An introduction to the application and future use of ^{234}Th in aquatic systems. *Mar. Chem.* **100**, 166–189.

Webster I. T., Hancock G. J. and Murray A. S. (1995) Modeling the effect of salinity on radium desorption from sediments. *Geochim. Cosmochim. Acta* **59**, 2469–2476.

Zohary T. (2004) Changes to the phytoplankton assemblage of Lake Kinneret after decades of a predictable, repetitive pattern. *Freshwater Biol.* **49**, 1355–1371.

Zukin J. G., Hammond D. E., Ku T.-L. and Elders W. A. (1987) Uranium–thorium series isotopes in brines and reservoir rocks from two deep geothermal well holes in the Salton Sea geothermal field, southeastern California. *Geochim. Cosmochim. Acta* **31**, 2719–2731.

Associate editor: John Crusius